Constraining the IMF in Extreme Environments: Detecting Young Low Mass Stars in Unresolved Starbursts

Michael R. Meyer and Julia Greissl

Steward Observatory, The University of Arizona, Tucson, AZ
contact: mmeyer@as.arizona.edu

ABSTRACT

We demonstrate the feasibility of detecting directly low mass stars in unresolved super–star clusters with ages < 10 Myr using near–infrared spectroscopy at modest resolution (R $\sim$ 1000). Such measurements could constrain the ratio of high to low mass stars in these extreme star–forming events, providing a direct test on the universal nature of the initial mass function (IMF) compared to the disk of the Milky Way (Chabrier, 2003). We compute the integrated light of super–star clusters with masses of 10^6 $M_\odot$ drawn from the Salpeter (1955) and Chabrier (2003) IMFs for clusters aged 1, 3, and 10 Myr. We combine, for the first time, results from Starburst99 (Leitherer et al. 1999) for the main sequence and post–main sequence population (including nebular emission) with pre–main sequence (PMS) evolutionary models (Siess et al. 2000) for the low mass stars as a function of age. We show that $\sim$ 4–12 % of the integrated light observed at 2.2 μm comes from low mass PMS stars with late–type stellar absorption features at ages < 3 Myr. This light is discernable using high signal–to–noise spectra (> 100) at R=1000 placing constraints on the ratio of high to low mass stars contributing to the integrated light of the cluster.

Subject headings: stars: mass function — pre–main sequence — formation; galaxies: starburst

1. Introduction

The observed initial mass function of stars, averaged over space and time in the disk of the Milky Way [1], provides a fundamental test for any theory of star formation. Characteristic masses (such as the transition from a power–law IMF to a log–normal form, as well as a

[1] See for example the review of Chabrier (2003) and references therein.

mean mass) provide evidence for preferred scales of star formation (Adams and Fatuzzo, 1996; Larson, 1985; 2005). The stellar IMF observed in nearby (< 1 kpc) star–forming regions appears to be broadly consistent with having been drawn from the field star IMF (Meyer et al. 2000). As a result, astronomers have been forced to look for differences either at very low masses (e.g. Briceno et al. 2002) or more extreme galactic star–forming environments (e.g. Figer et al. 1999).

Studies of starburst galaxies, with star formation rates orders of magnitude higher than normal disk galaxies (e.g. Kennicutt, 1998), have led to claims of IMFs distinct from that characterizing the disk of the Milky Way. For example, Smith and Gallagher (2001) find that some massive clusters in M82 exhibit a "low mass cut–off". However, Förster Schreiber et al. (2003; see also McCrady et al. 2005; Rieke et al. 1993) find a power–law slope for stars > 10 $M_\odot$ with a flattening at masses < 1.0 $M_\odot$ similar to the IMF of Chabrier (2003; see also Kroupa, 2001). Recent studies of the integrated light of super–star clusters forming in interacting galaxies suggest variations in mass–to–light ratios that could be interpreted as variations in the IMF (Mengel et al. 2002). Since such systems might be analogues for the vigorous star formation thought to have occurred in the early universe (e.g. Madau et al. 1996) it is particularly important to understand whether the IMF varies with metalicity or star–formation rate.

In order to: 1) provide important constraints on theories of star formation under extreme conditions; and 2) test claims of variations in the IMF for starburst galaxies and super–star clusters, we explore the feasibility of detecting directly the low mass pre–main sequence stars in young stellar populations. In section II, we outline our approach to simulating the integrated near–IR light from very young rich star–forming events. In section III, we discuss our results as a function of input model assumptions, and in section IV we discuss the uncertainties in constraining the ratio of high to low mass stars using the technique described here.

2. The Approach

We have simulated the integrated near–infrared spectrum from a stellar population using the assumptions outlined below. First, we assume single star–forming events with total mass 10^6 $M_\odot$ populated in Monte Carlo fashion by either a Salpeter (1955; hereafter S55) or Chabrier (2003; hereafter C03) IMF from 0.1–100 $M_\odot$ at ages of 1, 3, and 10 Myr. We take into account the effects of main sequence and post–main sequence evolution using Starburst99 (Leitherer et al. 1999). This program also includes nebular emission that results from interaction of the ionizing flux from the most massive stars formed with the surrounding

medium as it evolves along with the ensemble radiation field. Because we are interested in detecting low mass stars directly as a fraction of the integrated light in the near–infrared, the high mass stars and nebular emission [2] simply provide a featureless continuum against which we wish to detect spectral features from late–type stars.

We also include, for the first time, the effects of *pre–main sequence* (PMS) evolution explicitly on the integrated light of the stellar population. We use the models of Seiss et al. (2000) to provide appropriate mass–luminosity relationships as a function of time over a broad range of stellar masses. For populations 1/3/10 Myr old, all stars $< 7/5/3$ $M_\odot$ are PMS respectively. This corresponds to 0.971/0.956/0.911 % of all stars with total masses of of approximately 0.69/0.63/0.51 $\times$ the cluster mass in the PMS component for 1/3/10 Myr respectively (assuming a Chabrier, 2003 IMF). We adopt tables of intrinsic colors and bolometric corrections as a function of effective temperature and spectral type from Cox (2000) and use these to estimate the contribution of each PMS star to the integrated J– (1.25 μm), H– (1.65 μm), and K–band (2.2 μm) light. For each star, a mass is assigned based on probabilities from the input IMF. For the assumed age, this translates into a temperature and bolometric luminosity. For the model temperature, a color and bolometric correction is adopted resulting in a calculated absolute M_J, M_H, and M_K magnitude. Based on this temperature, we select a continuum normalized SNR $\sim$ 50 spectrum at R=1000 from the library of Meyer (1996) with weighting according to its absolute flux to produce the integrated PMS spectrum for the low mass stars. We then combined the PMS spectrum with the appropriately flux–weighted continuum from Starburst99 for the high mass main sequence and post–main sequence stars, along with the nebular continuum to produce the total integrated spectrum of the population as a function of age (Figure 1).

3. The Results

The integrated PMS spectra shown in Figure 1 exhibit late–type features due to CaI at 2.26 μm and the first–overtone CO absorption at 2.29 and 2.32 μm (prominent in stars > K0) as well as features of MgI at 2.28 μm (seen in stars from F2–M1) as noted by Ali et al. (1995), Hinkle and Wallace (1997), and Kleinmann and Hall (1986). While these features are difficult to see against the continuum of the high mass stars and nebular emission, they are detected at the 1 % level in high signal–to–noise ratio spectra. Table 1 shows the breakdown of relative flux in the J–, H–, and K–bands as a function of age and input IMF. The nebular continuum dominates at the youngest ages and becomes less important with time (Leitherer

[2] Dominated by free–free emission with a characteristic spectrum of $F_\lambda \sim \lambda^{-2}$.

et al. 1995). However, the low mass stars are also brightest at the youngest ages due to their PMS nature, partially off–setting the effect of strong nebular continuum. It appears that the low mass PMS stars contribute a roughly constant fraction to the integrated K–band flux from < 1 to > 3 Myr (> 0.07 to < 0.04 for the Chabrier (2003) IMF) though this effect is commonly ignored. Once the most massive stars evolve to become M supergiants at an age of ~ 8 Myr years, they dominate the continuum and the PMS stars become < 1 % of the integrated K–band flux making them almost impossible to detect. However, at ages $<$ 8 Myr, the low mass stars are detectable through the CO absorption features against the continuum of the high mass stars and nebular continuum.

We have investigated the diagnostic power of the spectral features indicated in Figure 1 by measuring the equivalent width of the features as a function of age and input IMF using the SPLOT routine within IRAF. Variations in determining the local continuum for each spectral feature provide the error estimates in the equivalent widths. As can be seen in Table 2, the combined strength of the (CaI+CO) indices, which are dominated by stars cooler than 3500 K and less than 0.5 $M_{\odot}$ from ages 1–3 Myr (Siess et al. 2000), decrease by factors of 2.13 (S55) and 3.28 (C03) as the populations age and the low mass stars become less luminous. Note that the combined index evolves more from 1–3 Myr for C03 (shallower IMF) compared to S55 since it is more sensitive to stars 0.2–0.5 $M_{\odot}$, whose luminosities are evolving faster than the stars < 0.2 $M_{\odot}$. The MgI index, tracing stars with temperatures between 3700–7000 K, is the same for both IMFs at 1 Myr where it is dominated by stars $>$ 1.0 $M_{\odot}$ (Siess et al. 2000): at high masses the IMF slopes are the same. Again because this index is dominated by higher mass stars from the C03 IMF whose luminosities are changing faster, it changes more from 1–3 Myr compared to S55 (factors of 3.36 versus 2.61). Note that the mass range sampled by the MgI feature, attributed to warmer stars compared to the CaI+CO index, decreases with time from with the upper mass limit going from 4 $M_{\odot}$ (1 Myr) to 2.5 $M_{\odot}$ (3 Myr). While the equivalent width ratio given in the last column of Table 2 $(EW[CaI]+EW[CO2-0)])/EW[MgI]$ does not evolve significantly from 1–3 Myr for the Chabrier (2003) IMF, both values are distinguished from the range of values realized from the S55 IMF. The difference between the 1 Myr S55 value and the 3 Myr old C03 value is $8.98 \pm 0.82 - 6.44 \pm 0.30 = 2.54 \pm 0.87$. Although the SNR of the spectra required in order to accurately measure the weak MgI feature probably exceeds 300 at R = 1000, our simulations suggest that we can distinguish between the C03 and S55 IMFs at the ~ 3 σ level provided we can estimate the age of the stellar population to within a factor of three.

4. The Discussion

We have demonstrated that, given our model assumptions are correct, it should be possible to discern the presence of the low mass stars in a very young unresolved stellar population. This would place important constraints on the ratio of high to low mass stars, and thus the IMF, in extreme star–forming environments. We now examine how sensitive the conclusions presented above are to the assumptions we have made. Would utilizing different PMS evolutionary calculations make a difference? Replacing the mass–luminosity–temperature relationships of Siess et al. (2000) as a function of age with those of Palla and Stahler (2000) or D'Antona Mazzitelli (1994) would result in a change of < 10 % in the absolute K–band magnitude of a 1 $M_{\odot}$ star at an age of 1 Myr. While there are larger uncertainties in the PMS evolutionary models at lower masses (e.g. Hillenbrand and White, 2004), the qualitative behavior of the models within our simulations will be the same.

We have assumed that Starburst99 correctly predicts the amount of nebular continuum for the unresolved population. The prescription used is described in Leitherer et al. (1995) and assumes that all ionizing photons contribute with high efficiency to producing the observed free–free emission. We considered the effects of changing the maximum stellar mass from 100 $M_{\odot}$ to 130 and 200 $M_{\odot}$ in our model stellar clusters. Moving the maximum mass to 130 $M_{\odot}$ made only a 1.3 % decrease to our prediction for the integrated K–band contribution from PMS stars to 5.7 % (increasing the continuum dilution of the late–type absorption features), while increasing the maximum mass to 200 $M_{\odot}$ decreased the integrated K–band light to 5.4 % for a 1 Myr old population assuming a Chabrier (2003) IMF (cf. Table I). Oey and Clarke (2005) have presented evidence for a universal maximum stellar mass between 120–200 $M_{\odot}$ while Figer (2005) suggests a maximum observed stellar mass of 130 $M_{\odot}$ based on observations of the Arches cluster (see Massey, 1999 for an alternative point of view). Further, if, as is observed in some star–forming complexes, the HII region has broken out of the molecular cloud over an appreciable solid angle, the estimated free–free continuum is an upper limit, making our predicted line strengths for low mass stars a lower limit.

We have also neglected the presence of circumstellar disks which could produce an additional veiling continuum further diluting the observed late–type stellar features from low mass stars. However, not all young stellar objects exhibit excess continuum emission at 2.3 μm and typical excess emission appears to peak at longer wavelengths (Meyer et al. 1997; Muzerolle et al. 2003). Further we have also underestimated the absorption line strength of the CO feature, which is surface gravity sensitive, as we have used higher gravity dwarf star templates to represent lower gravity PMS objects. These two effects tend to cancel. How does our choice of R=1000 affect the detectable of the low mass stars? While lower spectral resolution might make it easier to detect the spectral features (Nyquist sampled at R $>$ 300)

at the required SNR, it may be important to obtain higher resolution spectra in order to constrain the surface gravity of the dominant stellar population responsible for the stellar absorption. If any supergiant stars contribute to the integrated light observed at 2.3 μm, R < 3000 spectra should enable their identification due to the extremely low surface gravity, to which CO is sensitive (Aaronson et al. 1978; Meyer et al. 1998). In this preliminary work, we have ignored the effects of metalicity. Starburst galaxies are thought to have higher than solar metalicity, which would increase the absorption line strengths predicted in our simulations.

One degeneracy in constraining the slope of the IMF with which we must contend is that between the ratio of high to low mass stars and the luminosity of the PMS population as a function of age (see Table 1). If one assumed an age of 3 Myr for what was actually a 1 Myr old cluster, one might erroneously favor a steeper IMF (e.g. S55) rather than a C03 IMF based on analysis of the Ca+CO absorption strength alone. However, the line ratio analysis outlined above can distinguish between IMFs with powerlaw indices that differ by ~ 1.0 dex above and below 1 $M_{\odot}$ (e.g. between S55 and C03) provided that the age of the stellar population can be constrained within a factor of $\times$ 3. Recent work on modelling the spectral energy distributions (SEDs) of starburst galaxies suggest that ages for them can be derived within factors of $\times$ 3 given $>$ four points on the SED including the U– and B–bands as well as near–IR data (Anders et al. 2004). In addition, it is vital to know whether or not the cluster might contain supergiants (corresponding to ages > 8 Myr) which will dominate the near–IR continuum once they appear. Vazquez and Leitherer (2005) present model SEDs for very young starbursts that indicate it is relatively straight–forward to distinguish clusters $<$ and > 10 Myr based on the energy emitted between 300–1000 $\mathring{A}$ despite the uncertainties in the theoretical models. Further, Gonźalez Delgado and Pérez (2000) show that results from SED modelling which include UV data agree well with other techniques and give a consistent age of 3 Myr for the stellar populations associated with the HII region NGC 604 in M 33.

How can we treat uncertainties in the level of free–free emission? Rather than rely on the model predictions outlined above for the relative ratios of nebular emission to stellar emission, it would be very valuable to constrain the amount of nebular emission through observations. Since free–free emission from such a young stellar population becomes increasingly dominant at longer wavelengths, one could measure the free–free emission directly at centimeter wavelengths where it is expected to dominate dust and compare the inferred amount in the near–IR to the predictions of Starburst99. Spatially resolved observations of the HII regions in M17 by Ando et al. (2002) indicate qualitative agreement between observed IR emission and predicted free–free emission extrapolated from centimeter observations. An additional check on this extrapolation would be the predicted reddening corrected Br γ line flux given

the observed free–free emission. If one is able to detect the weak MgI feature discussed above, the line ratio suggested in Table 2 would render the measurement insensitive to uncertainties in the continuum veiling due to free–free emission. Removal of the free–free contribution to the observed near–IR spectrum and a model of the integrated stellar spectrum would place a direct constraint of the ratio of high to low mass stars.

Such constraints are sensitive to the relative slope of the IMF between 10–100 $M_{\odot}$ and 0.1–1.0 $M_{\odot}$, crucial for precise estimates of the mass–to–light ratios for older stellar populations. Is this observational approach feasible? Several candidate super–star clusters found in the overlap region of the interacting galaxy pair NGC 4038/39 exhibit weak CO absorption and are thought to be < 10 Myr old (Mengel et al. 2002) indicating that they lack late–type supergiants. These targets have K–band magnitudes between $14^m < K < 16^m$ (Kassin et al. 2003). We estimate that it would take $\sim$ 10 hours at R $\sim$ 1000 to obtain SNR $\sim$ 300 in the K–band to detect late–type features from low mass stars in a $K \sim 14^m$ young super–star cluster on an 8 meter telescope. Added information available through spectral observations in the J– and H–bands may make application of this technique easier. Despite all the caveats listed above, we believe the experiment is worthwhile, given the important implications of the observations.

We would like to thank the Claus Leitherer for the helpful suggestion that we investigate the effects of free–free emission on the integrated spectra of starbursts at young ages, as well as an anonymous referee for suggestions that improved the presentation of this paper. We also thank the organizers of the IMF@50 conference (Evidge Corbelli, Franscesco Palla, and Hans Zinnecker) for the opportunity to present a preliminary version of this work at the Abetto de Spinoza, and Morten Andersen along with Kelsey Johnson for comments on a draft of the paper. We gratefully acknowledge the support of a Cottrell Scholar award from the Research Corporation as well as NASA grant GO–9846 from the Space Telescope Science Institute.

REFERENCES

Aaronson, M., Persson, S. E., & Frogel, J. A. 1978, ApJ, 220, 442

Adams, F. C., & Fatuzzo, M. 1996, ApJ, 464, 256

Ali, B., Carr, J. S., Depoy, D. L., Frogel, J. A., & Sellgren, K. 1995, AJ, 110, 2415

Anders, P., Bissantz, N., Fritze-v. Alvensleben, U., & de Grijs, R. 2004, MNRAS, 347, 196

Ando, M., Nagata, T., Sato, S., Mizuno, N., Mizuno, A., Kawai, T., Nakaya, H., & Glass, I. S. 2002, ApJ, 574, 187

Briceño, C., Luhman, K. L., Hartmann, L., Stauffer, J. R., & Kirkpatrick, J. D. 2002, ApJ, 580, 317

Chabrier, G. 2003, PASP, 115, 763

Cox, A. N. 2000, Allen's astrophysical quantities, 4th ed. Publisher: New York: AIP Press; Springer, 2000.

D'Antona, F., & Mazzitelli, I. 1994, ApJS, 90, 467

Figer, D. F. 2005, Nature, 434, 192

Figer, D. F., Kim, S. S., Morris, M., Serabyn, E., Rich, R. M., & McLean, I. S. 1999, ApJ, 525, 750

Förster Schreiber, N. M., Genzel, R., Lutz, D., & Sternberg, A. 2003, ApJ, 599, 193

González Delgado, R. M., & Pérez, E. 2000, MNRAS, 317, 64

Hillenbrand, L. A., & White, R. J. 2004, ApJ, 604, 741

Kassin, S. A., Frogel, J. A., Pogge, R. W., Tiede, G. P., & Sellgren, K. 2003, AJ, 126, 1276

Kennicutt, R. C. 1998, ARA&A, 36, 189

Kleinmann, S. G., & Hall, D. N. B. 1986, ApJS, 62, 501

Kroupa, P. 2001, MNRAS, 322, 231

Larson, R. 2005, MNRAS, in press (astro-ph/0411737)

Larson, R. B. 1985, MNRAS, 214, 379

Leitherer, C., & Heckman, T. M. 1995, ApJS, 96, 9

Leitherer, C., et al. 1999, ApJS, 123, 3

Madau, P., Ferguson, H. C., Dickinson, M. E., Giavalisco, M., Steidel, C. C., & Fruchter, A. 1996, MNRAS, 283, 1388

Massey, P. 1999, IAU Symp. 190: New Views of the Magellanic Clouds, 190, 173

Mengel, S., Lehnert, M. D., Thatte, N., & Genzel, R. 2002, A&A, 383, 137

McCrady, N., Graham, J. R., & Vacca, W. D. 2005, ApJ, 621, 278

Meyer, M. R. 1996, PASP, 108, 380

Meyer, M. R., Calvet, N., & Hillenbrand, L. A. 1997, AJ, 114, 288

Meyer, M. R., Edwards, S., Hinkle, K. H., & Strom, S. E. 1998, ApJ, 508, 397

Meyer, M. R., Adams, F. C., Hillenbrand, L. A., Carpenter, J. M., & Larson, R. B. 2000, Protostars and Planets IV, 121

Muzerolle, J., Calvet, N., Hartmann, L., & D'Alessio, P. 2003, ApJ, 597, L149 Oey, S. & Clarke, C. 2005, ApJ, in press (http://xxx.lanl.gov/abs/astro-ph/0501135).

Palla, F., & Stahler, S. W. 2000, ApJ, 540, 255

Rieke, G. H., Loken, K., Rieke, M. J., & Tamblyn, P. 1993, ApJ, 412, 99

Smith, L. J., & Gallagher, J. S. 2001, MNRAS, 326, 1027

Salpeter, E. E. 1955, ApJ, 121, 161

Siess, L., Dufour, E., & Forestini, M. 2000, A&A, 358, 593

Vázquez, G. A., & Leitherer, C. 2005, ApJ, 621, 695

Wallace, L., & Hinkle, K. 1997, ApJS, 111, 445

Fig. 1.— Integrated spectra for a 10^6 $M_\odot$ cluster distributed from 0.1–100 $M_\odot$ via the S55 IMF for ages of 1 and 3 Myr compared to similar spectra derived from the C03 IMF at comparable ages based on the mass-luminosity relationships of Seiss et al. (2000). Late–type features due to the presence of low mass pre–main sequence stars, visible at the 1 % level against the light of the higher mass main sequence stars and nebular continuum, are noted. The presence of residual telluric absorption at 2.3150 μm is also indicated.

Table 1: Fraction of Integrated PMS Light for 10^6 M$\odot$ Cluster

Band	IMF[1]	τ (age)	F_{PMS}[2]	F_{MS}	F_{NEB}
J	S55	1 Myr	0.13	0.17	0.70
H	S55	1 Myr	0.175	0.125	0.70
K	S55	1 Myr	0.12	0.07	0.81
J	C03	1 Myr	0.09	0.18	0.73
H	C03	1 Myr	0.10	0.14	0.76
K	C03	1 Myr	0.07	0.07	0.86
J	C03	3 Myr	0.04	0.44	0.52
H	C03	3 Myr	0.05	0.37	0.58
K	C03	3 Myr	0.04	0.23	0.73
J	C03	10 Myr	0.01	0.99	0.00
H	C03	10 Myr	0.01	0.99	0.00
K	C03	10 Myr	0.01	0.99	0.00

[1] S55 indicates Salpeter (1955) and C03 indicates Chabrier (2003) IMF.

[2] Pre–main sequence mass–luminosity taken from Seiss et al. (2000).

Table 2: Equivalent Widths of Late–Type Features Visible in Integrated Spectra

IMF[1]	τ (age)	$EW[CaI]$[2]	$EW[MgI]$[2]	$EW[CO(2-0)]$[2]	$(EW[CO(2-0)] + EW[CaI])/EW[$
S55	1 Myr	0.3168 ± 0.0188	0.1092 ± 0.0090	0.6632 ± 0.0322	8.98 ± 0.82
S55	3 Myr	0.1515 ± 0.0083	0.0418 ± 0.0011	0.3090 ± 0.0114	11.01 ± 0.44
C03	1 Myr	0.2055 ± 0.0067	0.1150 ± 0.0079	0.5162 ± 0.0103	6.27 ± 0.44
C03	3 Myr	0.0640 ± 0.0016	0.0342 ± 0.0012	0.1558 ± 0.0062	6.44 ± 0.30

[1] S55 indicates Salpeter (1955) and C03 indicates Chabrier (2003) IMF.

[2] Equivalent widths in microns measured as described in the text.

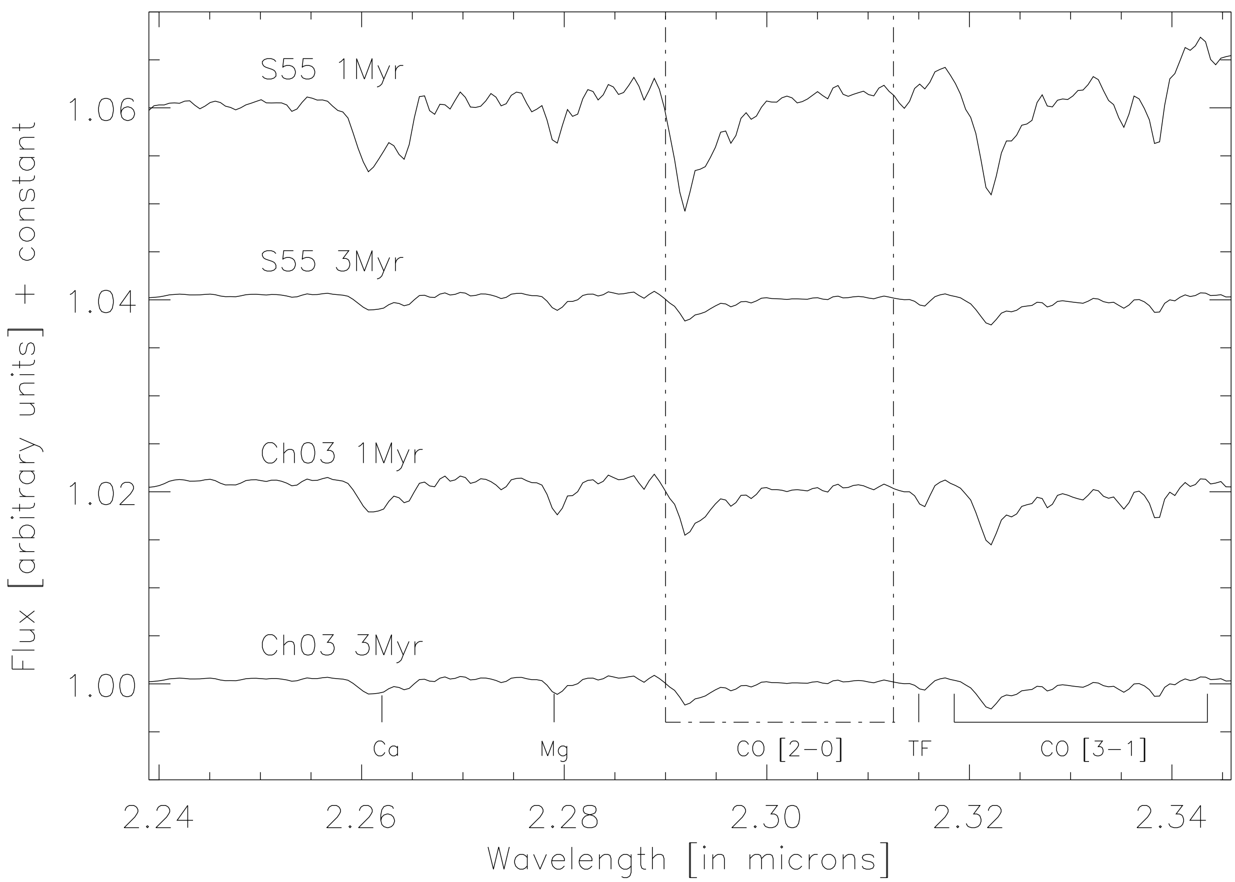
S55 1Myr
S55 3Myr
Ch03 1Myr
Ch03 3Myr
1.06
1.04
1.02
1.00
Flux [arbitrary units] + constant
Ca
Mg
CO [2-0]
TF
CO [3-1]
2.24
2.26
2.28
2.30
2.32
2.34
Wavelength [in microns]